Macroscopic inhomogeneities and the magnetoresistances of the simple metals

F. Paul Esposito, R. S. Newrock, and K. Loeffler
Physics Department, University of Cincinnati, Cincinnati, Ohio 45221
(Received 7 December 1978)

We have determined the effects of large-scale voids on the high-field thermal magnetoresistance of simple metals, including the effects of the lattice conductivity. The calculations were performed by a Green's function approach and by a boundary-value method. We find that the presence of the lattice conduction causes large deviations from the linear term evident in the electrical magnetoresistivity. The thermal magnetoresistivity, both transverse and longitudinal, saturates in sufficiently strong fields. The deviation from linearity occurs for $10 \leq \omega_c \tau \leq 100$ depending upon the magnitude of k_g. The Righi-Leduc coefficient is determined and it is found that the voids cause a slight increase. The magnetoresistance anomalies of potassium cannot be explained by the presence of voids.

I. INTRODUCTION

It is well known that the electrical and thermal magnetoresistivities of the simple metals are in strong disagreement with the predictions of the semiclassical transport theory. According to the theory, the magnetic field dependence of the electrical and thermal magnetoresistivity tensors should be determined by the compensation and the topology of the Fermi surface.[1] For the simple metals (uncompensated, with closed, nearly-free-electron-like Fermi surfaces) the theory predicts that both the electrical and thermal, transverse and longitudinal magnetoresistances saturate, i.e., become magnetic field independent in strong fields ($\omega_c \tau \gg 1$). Instead, the transverse electrical magnetoresistivity increases with field, usually as a linear function of the applied field.[2-5] In all of these metals the Kohler slopes S (defined by $\Delta\rho/\rho = S\omega_c\tau$) range from 10^{-2}–10^{-4}, and vary in an erratic manner with the specimen fabrication and handling techniques. In the simple metals for which the longitudinal electrical magnetoresistivity has been measured,[4-6] it often is linear in field, although a quadratic behavior has been observed.[4]

Recently, several articles have been published concerning investigations of the thermal magnetoresistivity of potassium, the archetypical simple metal. These investigations show that the transverse thermal magnetoresistivity contains a term quadratic in the applied field, along with the linear term.[7-9] The longitudinal thermal magnetoresistivity appears to be strictly linear in field.[9] In addition, the erratic behavior that is so evident in the electrical case does not appear in the thermal case. The magnitudes of the thermal Kohler slopes are of the same order as the electrical Kohler slopes, but, for specimens of similar purity, are four to five times larger. It should also be noted that for both resistivities, the transverse Kohler slopes are generally 30% to 50% lower than the longitudinal Kohler slopes.

A variety of explanations has been presented to explain these large deviations from theory.[10] At this time the issue is far from resolved and there is no agreement as to whether or not the source of the problem is intrinsic or extrinsic. The problem is an important one; it is generally considered to be one of the most important unsolved problems in metal physics. In this article, we examine one of the proposed extrinsic theories, that of magnetoresistance effects due to sample inhomogeneities. In particular, we examine the effects of the lattice thermal conductivity upon the distortions in the thermal current flow which are created by the presence of a macroscopic sample inhomogeneity.

As mentioned above, it has long been known that the electrical magnetoresistivities of the simple metals are highly irreproducible in the sense that the magnitudes of the Kohler slopes vary in an unpredictable manner with specimen handling and fabrication techniques. Also, in potassium at least, the behavior of the electrical magnetoresistivity before the onset of the linear terms is extremely erratic; knees, quasisaturation, and negative magnetoresistance have been observed.[2,3] Indeed, it is the presence of such behavior that provides most of the rationale for the extrinsic theories, that is, those theories which assume the nonsaturation is spurious and due to external causes, and is not a bulk property of the metal. Of the various possibilities, two have received considerable study: probe (geometry) effects and specimen inhomogeneities. Geometrical magnetoresistivity effects have been thoroughly investigated by a number of authors.[11-14] Geometrical magnetoresistivity arises when the current distribution in a conductor becomes dependent on the magnetic field in a manner not solely determined by changes in the bulk magnetoresistivity tensor. Distortions in the current distribution always result in an in-

creased dissipation in the specimen. However, in certain circumstances, if the current is improperly injected or extracted from the specimen, or if the voltage probes are poorly placed, or if the aspect ratio is poorly chosen, these distortions can lead to various spurious results including an apparent reduction in the total resistivity, a linear magnetoresistivity, and even a negative magnetoresistivity. These factitous results are easily avoided by proper experimental techniques, including high-impedance current injection and extraction, the placement of voltage probes more than a specimen's width from the specimen's ends, and the use of proper aspect ratios. It is worth noting that, in potassium at least, a linear electrical magnetoresistivity has been observed in both single and polycrystalline specimens, in both long wires and short "matchstick" specimens, and has been observed in experiments which use probe and probeless measurement techniques. The evidence is overwhelming and indicates that the nonsaturation is neither a probe nor a geometry effect.

Recently, a number of authors noted that the irreproducibility in the data might be a sign of the presence of macroscopic inhomogeneities in the specimens. Such inhomogeneities can produce a linear magnetoresistance. In particular, Sampsell and Garland,[15] Stroud and Pan,[16] and others[17] have demonstrated theoretically that contraction voids and highly conducting inclusions will generate a linear electrical magnetoresistivity. This has been experimentally verified.[18] Thus the question naturally arises as to whether the ultimate source of the magnetoresistivity anomalies in the simple metals is to be found in the effects of sample inhomogeneities on the flow of current in a magnetic field. To obtain an answer to this question, we have calculated the effects of voids on the thermal magnetoresistivity of a simple, free-electron metal. Although a void is a rather gross form of inhomogeneity, a consideration of its effects offers several significant advantages: the calculations are simple and straightforward, the results found for such inhomogeneities should be representative of those for other forms of defects, and the results are easily subjected to experimental verification. Additionally, it is a realistic calculation; contraction voids can certainly appear in metals. If desired, the step to a consideration of conducting inclusions is a simple one.

There are two approaches which may be taken to determine the effects of voids on the resistivity in a magnetic field; a boundary-value approach and an effective-medium approach. The effective-medium approach has a long history and, for the zero-field case, has been studied extensively.[19] Many of the methods developed for that case can be carried over into studies of the magnetoresistivity. In general, some sort of mean-field theory is used to determine an effective conductivity tensor, under the assumption that the inhomogeneities are randomly distributed in the medium. This is the approach taken by Stroud and Pan[16] (among others) for the case of a conducting inclusion or void in a metal. The boundary-value problem approach is also very straightforward. Laplace's equation is solved under the appropriate boundary conditions and the effective conductivity determined by an integration of the dissipation over the specimen's volume. This approach is of value for the case of low defect density, where overlap effects can be neglected. In either case, the defects are defined as spatial regions in which the conductivity tensor differs from that of the bulk (examples of these, in addition to voids, might be dislocations, strain fields, and differently oriented crystallites). The general features of the current distortions due to an isolated inclusion have been discussed by a number of authors, including those mentioned above. For the case of voids, the boundary-value approach and the effective-medium approach yield identical results: the two electrical magnetoresistivities are linear in the applied magnetic field with Köhler slopes $S \approx O(1)f$, where f is the volume fraction of voids. In addition, for the case of spherical voids, the transverse Kohler slope is about 30% smaller than the longitudinal Köhler slope. This is also seen in the experimental data. To test these ideas, Beers *et al.*[18] have introduced cylindrical voids into pure indium specimens, and found that the linear magnetoresistivity was considerably enhanced by the presence of the voids, and also that the theoretical predictions were essentially correct. However, the total picture is still unclear, and the question of the source of the magnetoresistance anomalies is yet unanswered. To account for a Köhler slope as large as 10^{-2}, a volume fraction $f = 10^{-2}$ is required, a quantity which is not only extremely unlikely, but which has not been found by direct measurement.[20] However, the presence of other forms of inhomogeneities with such a large volume fraction is certainly within reason, e.g., strain fields. In addition, the problem presented by the thermal magnetoresistivity must be investigated. In particular, can voids (or other inhomogeneities) produce the large quadratic term seen in the transverse thermal magnetoresistivity? Do the voids enhance the already present quadratic term due to the lattice conductivity?[7-9] If, as has been suggested, the quadratic term presents a separate problem, either wholly due to the lattice conductivity[8,21] or, perhaps due to a probe effect or other measurement artifact, can we account for the fact that the thermal Köhler

slopes are four to five times as large as the electrical Köhler slopes?[7,9]

We have therefore investigated the effects of including a magnetic-field-independent lattice thermal conductivity in a free-electron thermal magnetoconductivity tensor. We have performed the calculation using both the boundary-value approach and the effective-medium approach. The former method has several advantages, primarily that by calculating directly the fields and currents, and by obtaining the entropy production per volume, $-\vec{J}_Q \cdot \vec{\nabla}(1/T)$, the essential physics is observed easily. However, the effective magnetoresistance is tedious to obtain and requires a lengthy computer calculation. The effective-medium approach yields directly the effective resistivity and the Hall coefficient. Thus the two methods complement one another.

Our major results may be briefly stated. We demonstrate that the presence of voids does *not* enhance the quadratic term and that a nonzero lattice conductivity substantially reduces the effects of the voids in creating a linear thermal magnetoresistivity, producing also a marked deviation from linearity at high fields.

The rest of this paper is divided into four sections. In Sec. II we discuss the theoretical problem; in Sec. III we display the results for the various geometries; and in Sec. IV we discuss the application to real metals.

II. THEORY

In calculating the effects of voids on the thermal magnetoresistance, we use the complementary methods of Sampsell and Garland,[15] and Stroud and Pan.[16] As mentioned above, the method of Sampsell and Garland directly produces the fields and currents due to the presence of voids and presents a clear picture of the distortions caused by them. However, it is only after rather extensive machine calculations that the effective resistivity of the sample emerges. We still use the method of Stroud and Pan to calculate the effective resistivity. The combination of the two methods allows ease of computation, physical insight, and application to other problems, which otherwise would not have been either possible or as complete. We will first describe the calculations of the fields and currents for various void geometries and field orientations, leaving the full expressions for the Appendix. Next, we will present a rather direct calculation of the effective resistivity.

At the start, we make the assumptions that the metal is described by a free-electron model, that the mean-free-path of the electrons is much smaller than the void size which is in turn much smaller than the sample. These assumptions allow us to use continuum physics to describe the electrons. We also assume that the temperature is sufficiently low so that radiation effects may be neglected. This ensures the same boundary conditions for the electrical and the thermal currents and potentials. Furthermore, we assume that there is a field-independent lattice thermal conductivity present.

Since there are no heat sources present, by conservation of energy we have

$$\nabla_i J_Q^i = 0 , \tag{1}$$

where J_Q^i is the thermal current. In the presence of a magnetic field, this equation has the form

$$\nabla_i \kappa^{ij} \nabla_j T = 0 , \tag{2}$$

with $T(x,y,z)$ the temperature distribution. We have used the constitutive relation

$$J_Q^i = -\kappa^{ij} \nabla_j T , \tag{3}$$

whose inverse is written

$$\nabla_i T = - W_{ij} J_Q^j , \tag{4}$$

where κ^{ij} is the thermal conductivity tensor, and W_{ij} is the thermal resistivity tensor. When the conductivity tensor does not depend on the coordinates, Eq. (2) reduces to

$$\kappa^{ij} \nabla_i \nabla_j T = 0 \tag{5}$$

from which we see that the temperature distribution is determined solely by the symmetric part of the thermal conductivity tensor. For the model described above, the conductivity tensor takes the form

$$\kappa^{ij} = \kappa_0 \begin{bmatrix} \gamma + \delta & \beta\gamma & 0 \\ -\beta\gamma & \gamma + \delta & 0 \\ 0 & 0 & 1 + \delta \end{bmatrix} , \tag{6}$$

where κ_0 is the free-electron thermal conductivity in zero field, δ is the ratio of the lattice thermal conductivity to the free-electron thermal conductivity, $\gamma = (1+\beta^2)^{-1}$, $\beta = \omega_c \tau_{\text{th}}$, ω_c is the cyclotron frequency, and τ_{th} is the mean time between collisions catastrophic to thermal conduction. T does not satisfy Laplace's equation in the original coordinate system, i.e., Eq. (5) with the choice for κ^{ij} given by Eq. (6) is not Laplace's equation and, indeed, is not so even when the lattice conductivity is absent. It is always possible to find a coordinate system in which T does satisfy Laplace's equation. We let the original coordinate system be the unprimed system. Then the coordinate transformation which reduces Eq. (5) to Laplace's equation has the Jacobian

$$\frac{\partial x^{i'}}{\partial x^{j}} = \begin{bmatrix} 1 & 0 & 0 \\ 0 & 1 & 0 \\ 0 & 0 & \Gamma^{1/2} \end{bmatrix}, \tag{7}$$

where

$$\Gamma = (\gamma + \delta)/(1 + \delta). \tag{8}$$

The thermal conductivity tensor in the new system is easily calculated,

$$\kappa^{i'j'} = \Gamma^{-1/2} \frac{\partial x^{i'}}{\partial x^{i}} \frac{\partial x^{j'}}{\partial x^{j}} \kappa^{ij} \tag{9}$$

$$= \Gamma^{-1/2} \tilde{\gamma} \kappa_0 \begin{bmatrix} 1 & \tilde{\beta} & 0 \\ -\tilde{\beta} & 1 & 0 \\ 0 & 0 & 1 \end{bmatrix}, \tag{10}$$

where

$$\tilde{\gamma} = \gamma(1+\rho), \quad \tilde{\beta} = \beta(1+\rho)^{-1}, \text{ and } \rho = \delta\gamma^{-1}. \tag{11}$$

We make yet another coordinate transformation to a set of coordinates, the twiddled coordinates, $\tilde{x}^i$, appropriate to the specific geometry of the void. For the calculations in this paper, we choose ellipsoidal cylindrical coordinates for the cylindrical void, and oblate spheroidal coordinates for the spherical void. In these coordinate systems, the solutions to Laplace's equations are elementary, the appropriate boundary conditions easily imposed, and thus the temperature distributions uniquely determined. The boundary conditions are that the thermal current is injected uniformly at a great distance from the void, either perpendicular or parallel to an imposed uniform magnetic field, and that the component of the thermal current normal to the surface of the void is zero. Having determined the temperature distribution in the twiddled coordinates, $\tilde{T}$, we may now transform it and the currents back to the original coordinates, according to the following obvious relations:

$$\nabla_i T = \frac{\partial x^{i'}}{\partial x^{i}} \frac{\partial \tilde{x}^{k}}{\partial x^{i'}} \frac{\partial \tilde{T}}{\partial \tilde{x}^{k}}, \tag{12}$$

and

$$J_Q^i = \Gamma^{1/2} \frac{\partial x^{i}}{\partial x^{i'}} \frac{\partial x^{i'}}{\partial \tilde{x}^{k}} \tilde{J}_Q^k, \tag{13}$$

where

$$\tilde{J}_Q^i = -\tilde{\kappa}^{ij} \frac{\partial \tilde{T}}{\partial \tilde{x}^{j}} = -\frac{\partial \tilde{x}^{i}}{\partial x^{i'}} \frac{\partial \tilde{x}^{k}}{\partial x^{j'}} \kappa^{i'j'} \frac{\partial \tilde{T}}{\partial \tilde{x}^{k}}, \tag{14}$$

and where $\tilde{\kappa}^{ij}$ is the conductivity tensor in the geometry prescribed by the voids. In this paper, as mentioned above, we consider cylindrical voids with the magnetic field perpendicular to the axis of the void with a thermal current injected perpendicular or parallel to the field, and spherical voids with current injected perpendicular or parallel to the field. The expressions for the temperature distributions and thermal current are given in the Appendix.

We should mention also that the formalism described above can deal effectively with problems considerably more complicated than those discussed here. Equation (5), combined with a choice of κ^{ij} [for example, expression (6)], displays the physics of the model in as perspicuous a manner as possible. As observed above, T is determined by the symmetric part of κ^{ij}; antisymmetric modifications of κ^{ij} do not affect the temperature distribution. The symmetric part of κ^{ij} may always be diagonalized, and a rescaling of the coordinates reduces the equation for the temperature to Laplace's equation. This was the result used above.

While the temperatures and currents are easily derived, the effective resistivity of a sample is obtained only after extensive numerical calculation; the entropy production must be integrated over the volume of the sample. As an alternative to this procedure, we have found the method of Stroud and Pan[16] to be most efficient. The method is easy to describe, easy to use, and, for completeness, we include the application of the method to the problem at hand.

We begin by considering a solid of volume V, with a thermal conductivity tensor κ^{ij}. The volume is bounded by the outer surface ∂V and contains a volume fraction f of ellipsoidal inclusions each of which carries a conductivity tensor κ'^{ij}. We impose the boundary conditions that $n_i J_Q^i = n_i J_0^i$ on ∂V, where J_0^i is a constant current vector field, and n_i is normal to the surface ∂V. We now define, following Stroud and Pan, the effective thermal resistivity W_{ij}^{eff} of the system by the expression

$$\langle -\nabla_i T \rangle = W_{ij}^{\text{eff}} \langle J_Q^j \rangle, \tag{15}$$

where the brackets are taken to mean volume averages. Conservation of energy reduces Eq. (15) to

$$\langle -\nabla_i T \rangle = W_{ij}^{\text{eff}} J_0^j, \tag{16}$$

and we must now determine $\langle -\nabla_i T \rangle$. At this point, if we assume that the inclusions do not interact or, in other words, that the volume fraction of inclusions is small, we need keep only first order terms in f, and the calculation has been reduced to determining the effect of a single inclusion. This is easily done.

Following Stroud and Pan, we define

$$\tilde{\kappa}^{ij} = \begin{cases} \kappa'^{ij} \text{ in the inclusion}, \\ \kappa^{ij} \text{ elsewhere}, \end{cases} \tag{17}$$

and

$$\delta\kappa^{ij} = \kappa^{ij} - \kappa'^{ij}, \tag{18}$$

and, upon applying the variation operator to Eq. (2), we find that the effect of the inclusion on the temperature distribution, $\delta T = T - T^0 = T - (\nabla_i T^0)x^i$, is determined by the equation

$$\nabla_i \kappa^{ij} \nabla_j \delta T = -\nabla_i \delta\kappa^{ij} \nabla_j T . \tag{19}$$

Equation (19) has its Green's function, appropriate for the boundary conditions of the problem, given by

$$G(\vec{x},\vec{x}') = \frac{1}{4\pi(\kappa^{11}\kappa^{22}\kappa^{33})^{1/2}} \times \left(\frac{(x-x')^2}{\kappa^{11}} + \frac{(y-y')^2}{\kappa^{22}} + \frac{(z-z')^2}{\kappa^{33}}\right)^{-1/2} . \tag{20}$$

After integrating by parts and taking a gradient, we arrive at the result that the thermal field inside the void satisfies the equation

$$\nabla_i T^{\text{in}} = \nabla_i T^0 + \Gamma_{ij}(\kappa'^{jk} - \kappa^{jk})\nabla_k T^{\text{in}} , \tag{21}$$

where

$$\Gamma_{ij} = \oint \frac{\partial G(\vec{x},\vec{x}')}{\partial x'^i} n_j \, d^2x' \tag{22}$$

and the integral is over the surface of the inclusion. The effective thermal resistivity may now be determined as follows. Defining

$$\tilde{W}_{ij} = \begin{cases} W'_{ij} \text{ within the inclusion}, \\ W_{ij} \text{ elsewhere}, \end{cases} \tag{23}$$

we have

$$\langle -\nabla_i T\rangle = V^{-1}\int_v \tilde{W}_{ij} J_Q^j \, d^2x , \tag{24}$$

$$= W_{ij} J_0^j + f(W'_{ij} - W_{ij})\kappa'^{jk}\nabla_k T^{\text{in}} , \tag{25}$$

and using Eq. (21), we find

$$\langle -\nabla_i T\rangle = [W_{ij} - fW_{ij}(\kappa'^{jl} - \kappa^{jl})N_l^k W_{km}] J_0^m , \tag{26}$$

where

$$(N^{-1})_j^i = \delta_j^i - \Gamma_{jm}(\kappa'^{mi} - \kappa^{mi}) . \tag{27}$$

We have now isolated the effective thermal resistivity and it has the form

$$W_{ij}^{\text{eff}} = W_{ij} - fW_{ik}(\kappa'^{kl} - \kappa^{kl})N_l^m W_{mj} . \tag{28}$$

For cylindrical voids, $\kappa'^{ij} = 0$, the evaluation of the integrals in (22) yields

$$\Gamma_{11} = [\Gamma_{33} + (\kappa^{33})^{-1}](1-\epsilon)^{-1} , \tag{29}$$

$$\Gamma_{33} = [1 - (1-\epsilon)^{1/2}](\kappa^{33}\epsilon)^{-1} , \tag{30}$$

with $\epsilon = 1 - \kappa^{11}(\kappa^{33})^{-1}$, and all other integrals equal to zero. These are essentially identical to the results of Stroud and Pan for this geometry. The construction of the effective resistivity (28) is straightforward and we have

$$W_{11}^{\text{eff}} = W_{11} + f(W_{11} - \Gamma_{11}\kappa^{12}W_{21})(1+\Gamma_{11}\kappa^{11})^{-1} , \tag{31}$$

$$W_{33}^{\text{eff}} = W_{33} + fW_{33}(1+\Gamma_{33}\kappa^{33})^{-1} , \tag{32}$$

and

$$W_{12}^{\text{eff}} = W_{12} + f(W_{12} - \Gamma_{11}\kappa^{12}W_{22})(1+\Gamma_{11}\kappa^{11})^{-1} . \tag{33}$$

For spherical voids, $\kappa'^{ij} = 0$, Γ_{ij} has the nonvanishing components

$$\Gamma_{33} = [(1-\epsilon)^{1/2}(\sin^{-1}\epsilon^{1/2})/\epsilon^{1/2} - 1](\kappa^{33}\epsilon)^{-1} , \tag{34}$$

$$\Gamma_{11} = \Gamma_{22} = -\tfrac{1}{2}[\Gamma_{33} + (\epsilon\kappa^{11}\kappa^{33})^{-1/2}\sin^{-1}\epsilon^{1/2}] , \tag{35}$$

with $\epsilon = 1 - \kappa^{11}(\kappa^{33})^{-1}$. Using these expressions in Eq. (28), we find

$$W_{11}^{\text{eff}} = W_{11} + f[(1+\Gamma_{11}\kappa^{11})^2 + (\Gamma_{11}\kappa^{12})^2]^{-1} \times [(1+\Gamma_{11}\kappa^{11})W_{11} - \Gamma_{11}\kappa^{12}W_{21}] , \tag{36}$$

$$W_{33}^{\text{eff}} = W_{33} + fW_{33}(1+\Gamma_{33}\kappa^{33})^{-1} , \tag{37}$$

and

$$W_{12}^{\text{eff}} = W_{12} + f[(1+\Gamma_{11}\kappa^{11})^2 + (\Gamma_{11}\kappa^{12})^2]^{-1} \times [(1+\Gamma_{22}\kappa^{22})W_{12} - \Gamma_{11}\kappa^{12}W_{22}] . \tag{38}$$

A discussion of the expressions derived in this section follows.

III. RESULTS

In this section we describe the results of the calculations of Section II. Consistent with the conditions imposed on our calculations (low temperatures and the hydrodynamic limit), when we set the lattice conductivity to zero, our results are equivalent to those obtained by Sampsell and Garland, and Stroud and Pan for the electrical case; in the following discussion, our comments on the thermal resistivity for $\delta = 0$ apply with equal force to the electrical resistivity. These authors have given a thorough explanation of their results; in the discussion to follow, for completeness, we will briefly summarize the key points of their explanation. Our discussion is divided into three parts; we start with the transverse thermal magnetoresistivity, follow with the longitudinal thermal magnetoresistivity, and end with a brief discussion of the Righi-Leduc (thermal Hall) effect.

A. Transverse thermal magnetoresistivity

When the lattice conductivity is set to zero, a strong magnetic field will cause the thermal current flow to be severely distorted in the vicinity of the void. Significant distortions of the current streamlines extend to distances of the order $\omega_c\tau R_0$ in directions parallel to the magnetic field (R_0 is the radius of the void). The distortion in directions perpendicular to the field decreases as the field increases, so that in very high fields the

current lines do not "feel" the void until they enter its "shadow". [See inset, Fig. 1(a).] As indicated by Sampsell and Garland, a current sheet (for a cylindrical void) or a current shell (for a spherical void) is formed in the void's shadow (see Figs. 1, 2, and 4, in Ref. 15). These current sheets (or shells) flow nearly parallel to $\vec{H}$, up one side of the shadow and down the other. They are regions of intense dissipation; in fact, this dissipation is the major source of the extra resistivity which produces the linear term in the electrical magnetoresistivity ρ_{xx}.

In the thermal case, lattice conductivity has a dramatic effect on these current sheets and shells. We may see this by examining the volume entropy production as a function of the distance from a spherical void, Fig. 1. In this figure, we plot the volume entropy production versus the distance from the void along a line parallel to the x axis, perpendicular to $\vec{H}$, at a height $z = R_0$ [see inset, Fig. 1(a)]. Figure 1(a) shows the volume entropy production (or joule heating for $\delta = 0$) and is similar to Fig. 3 of Sampsell and Garland. Figure 1(b) shows the entropy production for $\delta = 10^{-4}$, a realistic value for the simple metals. These plots are normalized to unit volume entropy production (or joule heating) at distances far from the void and in low fields ($\omega_c\tau_{th} \ll 1$). (Additional curves for these cases were presented in an earlier Letter.[22])

At small $\omega_c\tau_{th}$, the magnetic field and the lattice conductivity have very little effect and the current distortions are due primarily to the obstructive effect of the void. We notice also that for small $\omega_c\tau_{th}$, the bulk conductivity tensor [Eq. (6)] is nearly isotropic. The maximum entropy production occurs at $x = 0$, where the current streamlines are bunched together as they pass around the void. For $\delta = 0$ [Fig. 1(a)], as $\omega_c\tau$ increases, peaks appear near $x = \pm R_0$. These peaks become more pronounced and narrower as $\omega_c\tau$ increases. The size of the peaks indicates an enormous dissipation in the void shadow. For $\delta \neq 0$, at large $\omega_c\tau_{th}$, the peak amplitude is slightly reduced and becomes less significant relative to an increasingly important background entropy production. The background entropy production represents the increased thermal magnetoresistance of the bulk due to the presence of lattice conduction.[21] The electronic thermal conductivity is sharply reduced as $\omega_c\tau_{th}$ increases [$\propto(\omega_c\tau_{th})^{-2}$], phonon conductivity becomes more significant, and the bulk resistivity in-

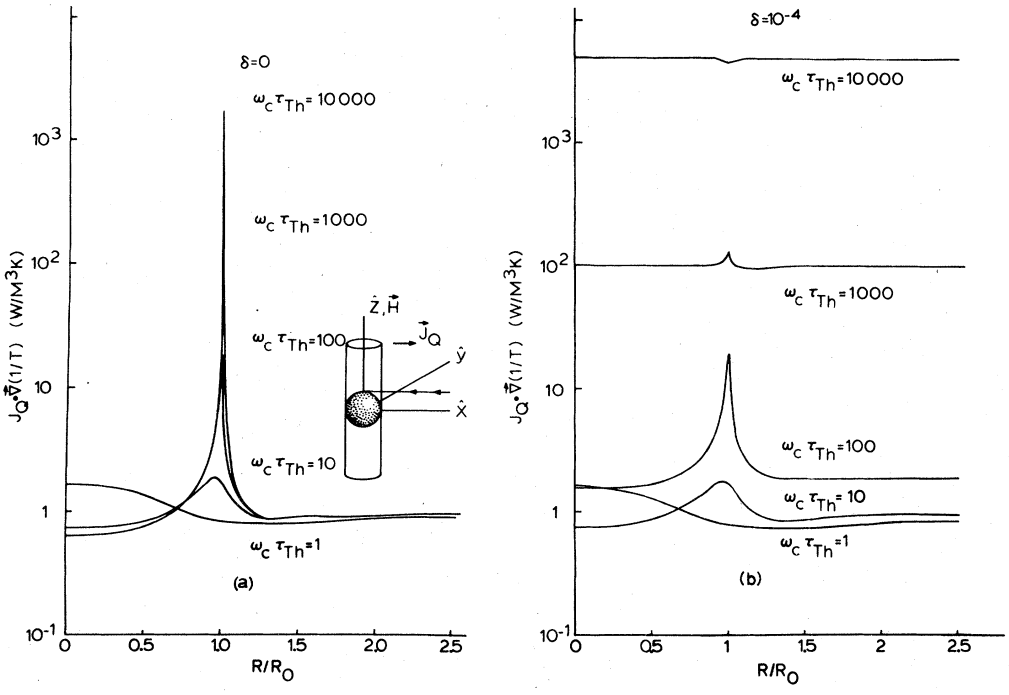

FIG. 1. Volume entropy production, $-\vec{J}_Q \cdot \vec{\nabla}(1/T)$, as a function of the distance from a spherical void along a line $z = R_0$ (see inset), $\vec{J}_Q \perp \vec{H}$. The entropy production is normalized to unity far from the void and in zero field. (a) $\delta = 0$. The large peak indicates the area of intense entropy production in the void shadow (see inset). Note that these curves can also be interpreted as the volume power density, $\vec{J} \cdot \vec{E}$, for the electrical case. (b) $\delta = 10^{-4}$. Notice the increase in the entropy production in the bulk and the disappearance of the peak (see text).

creases. At sufficiently large fields, phonon conductivity completely dominates the conductivity tensor, the thermal conductivity tensor is again isotropic, and little or no change in the dissipation occurs with increasing field. The voids again act simply as obstructions to the current flow. The above discussion holds for all values of δ, and a similar behavior is observed for the cylindrical voids.

The effects of the excess entropy production due to the presence of the void on the thermal magnetoresistivity is displayed in Figs. 2 and 3. These are Köhler plots of the "extra" thermal resistivity vs $\omega_c\tau_{th}$, where

$$\frac{\Delta W_{extra}}{W_0} = \frac{W_{calc}(H,T) - W_{no\,void}(H,T) - W_{extra}}{W_0} . \quad (39)$$

For this equation, W_{calc} is the thermal magnetoresistivity as calculated from Eq. (31) or (36). $W(H,T)_{no\,void}$ is the free-electron thermal magnetoresistivity in the absence of voids, W_{extra} is the added resistivity in zero field due to the presence of the void, and $W_0 = 1/\kappa_0$. (We do not normalize to the zero-field thermal resistivity in the presence of voids since we are only interested in effects which are first order in f.)

The results are shown in Fig. 2 for the cyclindrical case and Fig. 3 for the spherical case. (For these figures, f is chosen to be 0.01.) For $\delta = 0$, we obtain a linear thermal magnetoresistivity with a Köhler slope $S = 1.00f$ for the cylinder and $0.64f$ for the sphere, in agreement with Sampsell and Garland, and Stroud and Pan. When δ is not zero, the extra thermal magnetoresistivity is no longer a linear function of the field. For each value of δ, there is a departure from linearity at a relativity low value of $\omega_c\tau_{th}$; at very high fields, the thermal magnetoresistivity increases rapidly and then saturates at a value $\propto 1/\delta$.

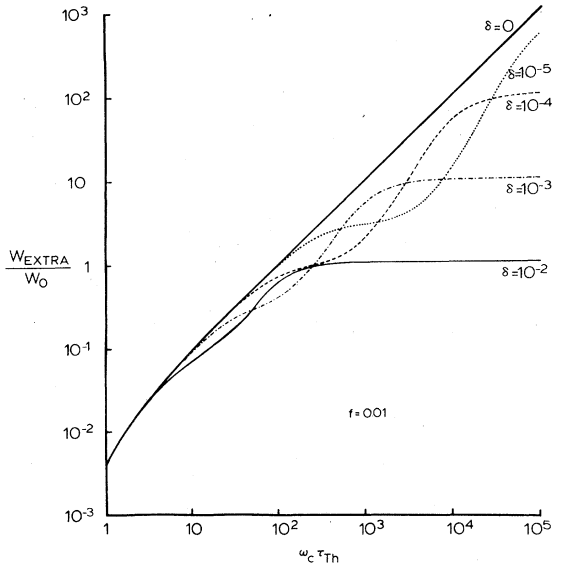

FIG. 2. Köhler plot of the extra transverse thermal magnetoresistivity (see text) vs $\omega_c\tau_{th}$ for a cylindrical void. For $\delta = 0$, the extra resistivity is linear in H for $\omega_c\tau_{th} \gtrsim 10$; this may also be interpreted as plot of the electrical magnetoresistivity, $\Delta\rho_{xx}/\rho_0$.

The departure from linearity occurs when the field is large enough so that phonon conduction is a significant fraction of the total conduction, or when $S \approx 0.1\gamma$. The very high field saturation value represents the "extra" resistivity due to the obstruction of the current flow. This region is reached when the electronic thermal currents are negligible. In the intermediate region the behavior is a result of the complicated interplay among competing conduction mechanisms.

B. Longitudinal thermomagnetoresistance

As shown in Refs. 15 and 16, spherical and cylindrical voids have the same net effect upon the longitudinal electrical magnetoresistance. We will discuss the more interesting case of the spherical void, where the current lines develop a pronounced circulation (see Fig. 4 in Ref. 15). For an electric current injected parallel to the magnetic field, the off-diagonal conductivity tensor elements become important when the perturbing effect of the void is sensed by the current. This produces a strong circulation. The current "corkscrews" toward the void in an expanding helix until it passes over the void and it repeats this behavior on the other side of the void, with a circulation in the opposite sense. Since the zz component of the conductivity tensor is relatively large in a magnetic field, these distortions persist to large distances

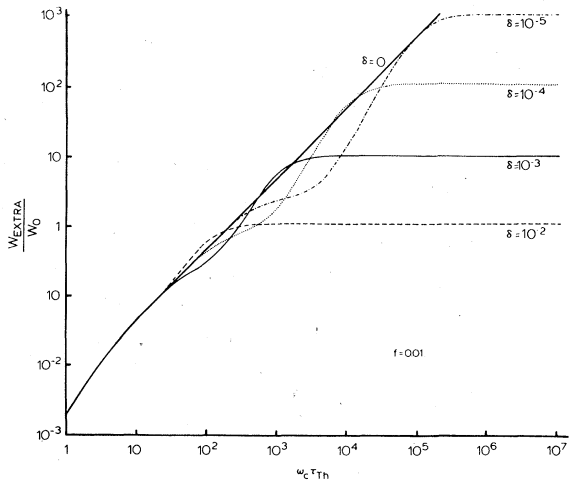

FIG. 3. Same as Fig. 2 for spherical voids.

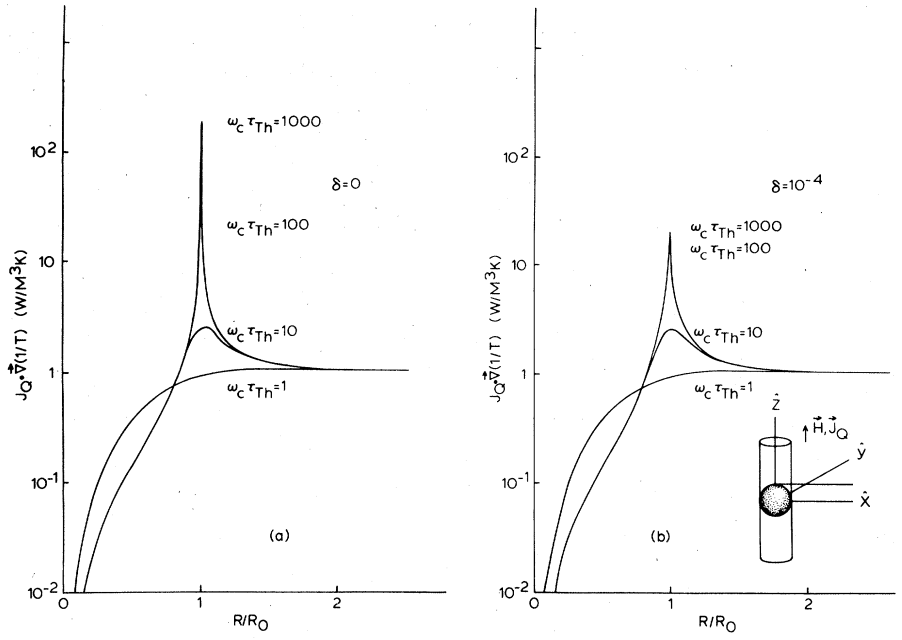

FIG. 4. Volume entropy production, $-\vec{J}_Q\cdot\vec{\nabla}(1/T)$, as a function of the distance from a spherical void in the plane $z=R_0$ (see inset), $\vec{J}_Q \| \vec{H}$. These curves show the entropy production on a line passing through the cylindrical void shadow. The entropy production is normalized to unity far from the void and in zero field. (a) $\delta=0$. These curves may also be interpreted as the electrical power dissipation $\vec{J}\cdot\vec{E}$. (b) $\delta=10^{-4}$.

from the void. The current lines form a thin shell when passing over the void and the dissipation in this shell causes the linear electrical magnetoresistivity or, in our case, an extra thermal magnetoresistivity. Again, as in the transverse case, lattice conduction has pronounced effects. In Figs. 4 and 5 we plot the volume entropy production for the longitudinal geometry for $\delta=0$ and $\delta=10^{-4}$. These curves display the volume entropy production as a function of the distance from the sphere for two cases: in Fig. 4 we move in along the void shadow, $x^2+y^2=1$, and in Fig. 5 we move across the void shadow, perpendicular to $\vec{H}$, $z=$constant [see insets in Figs. 4(b) and 5(b)]. As before, the curves are normalized to unit entropy production (or joule heating) far from the void and in small fields.

In low fields, the presence of the field or the lattice conductivity has little or no effect. A comparison of Figs. 4(a) and 5(a) shows that there is

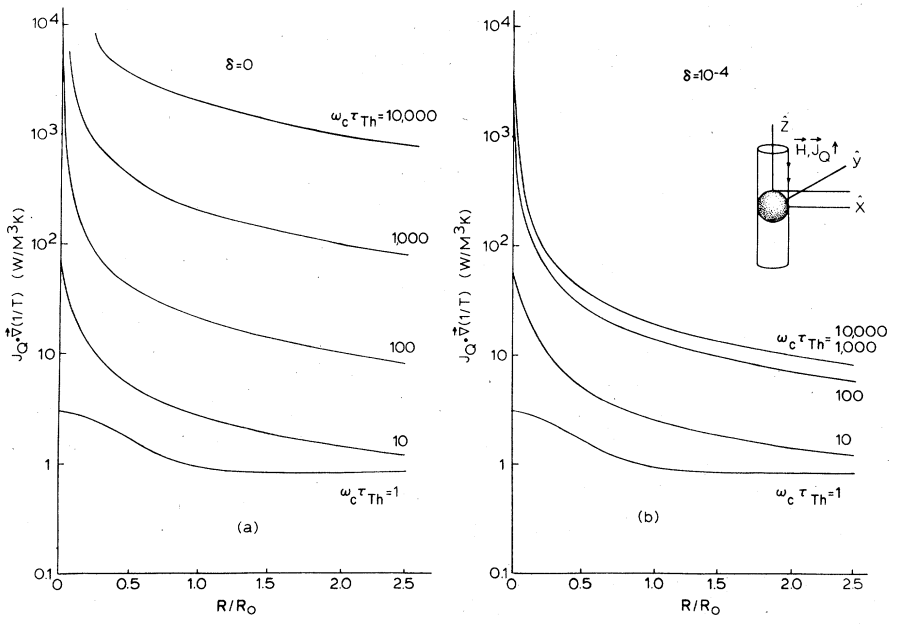

FIG. 5. Same as Fig. 4 for a line along the void shadow (see inset).

a small increase in the entropy production localized to regions very close to the void, where the current streamlines are squeezed together. This is again a simple obstruction effect. For $\delta = 0$, as $\omega_c\tau$ increases, a large peak forms, indicating a large increase in the entropy production. This region of increased entropy production is confined to the cylindrical void shadow. As $\omega_c\tau$ increases further, the peak height increases enormously and the distortions to the current lines produced by the void are seen farther and farther from the void, along the field direction. At the same time, the width of the shell decreases. The distortions and the increased entropy production persist to distances on the order of $\omega_c\tau R_0$.

The lattice conductivity has a very strong effect. As $\omega_c\tau$ increases [Figs. 4(b) and 5(b)], the peak in the entropy production still forms, indicating the presence of the current sheets. Eventually, however, a maximum amplitude is reached and further increases in $\omega_c\tau_{th}$ have no effect. The entropy production far from the void remains unchanged since the lattice conductivity does not create a bulk longitudinal thermal magnetoresistivity as it does in the transverse case. In the electrical case, the increasing dissipation in the void shadow as $\omega_c\tau$ increases yields an increasing electrical magnetoresistivity; we thus expect to see saturation in the extra thermal magnetoresistivity. Figure 6 shows the extra contribution to the thermal magnetoresistivity for the two cases. These are Köhler plots of $W_{\text{extra}}(H, T)$, as defined from Eq. (39) using Eqs. (32) and (37). These curves show a smooth departure from linearity and a smooth, steady rise to saturation. The saturation of the longitudinal thermal magnetoresistivity displayed here is due to a different mechanism than that which produces saturation in the transverse case. In the transverse case, the electronic part of the thermal conductivity tensor, κ_e^{xx}, decreases as $1/H^2$, leading, in very high fields, to a bulk thermal magnetoresistivity proportional to $1/\delta$. The saturation value of $(\Delta W_{\text{extra}}/W_0)_{\text{trans}}$ is simply that value due to the obstruction of the current by the void.

In the longitudinal geometry, there is no electrical or thermal magnetoresistivity in the absence of the void; the only effect of the lattice conductivity is a slight change in W_{zz} $[=1/\kappa^{33} = 1/(1+\delta)]$.

C. Righi-Leduc coefficient

Stroud and Pan show that spherical voids have a small effect on the Hall coefficient R_H. The change is an increase of $O(f)$, and R_H is essentially constant at high fields. Cylindrical voids have no effect on R_H in high fields. In the thermal case, the results are similar. In the bulk metal, lattice conduction produces a large deviation of the Righi-Leduc coefficient from the constant free-electron value,[23] $R_{\text{RL}} = 1/L_0 Tne$. The presence of cylindrical voids causes no additional effect. For spherical voids there is a low-field enhancement of about 2% (for $f = 0.01$, Fig. 7) which rapidly decreases with increasing $\omega_c\tau_{th}$ and then rises to a constant value at high fields. These effects are, however, quite small.

IV. DISCUSSION

In this section we discuss the results of Sec. III. We make comparisons to real metals, discuss how

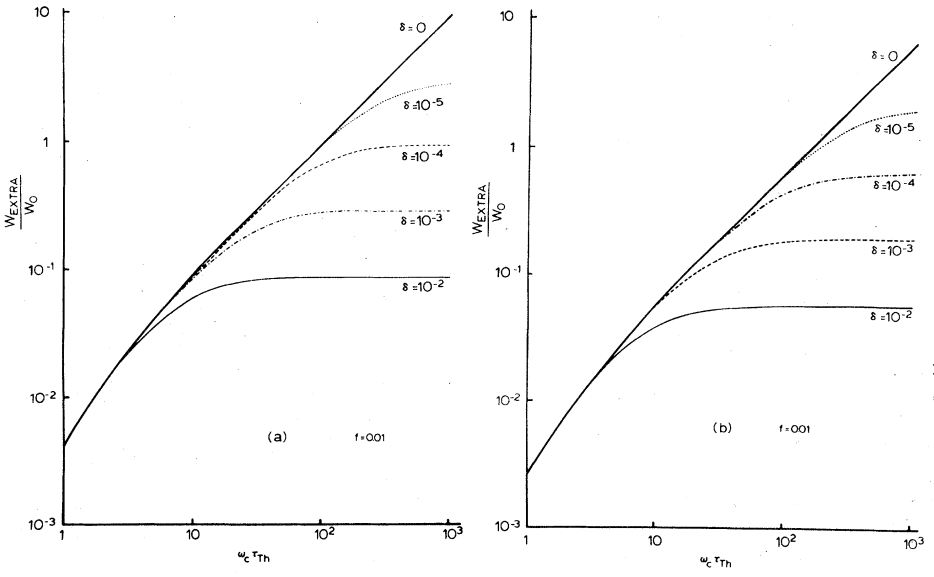

FIG. 6. Köhler plot of the extra longitudinal thermal magnetoresistivity (see text) vs $\omega_c\tau_{\text{th}}$ for (a) cylindrical voids and (b) spherical voids. For $\delta = 0$ the extra thermal resistivity is linear in field for $\omega_c\tau_{\text{th}} \lesssim 10$. This curve may also be interpreted as the longitudinal electrical magnetoresistivity $\Delta\rho_{xx}/\rho_0$ vs $\omega_c\tau$.

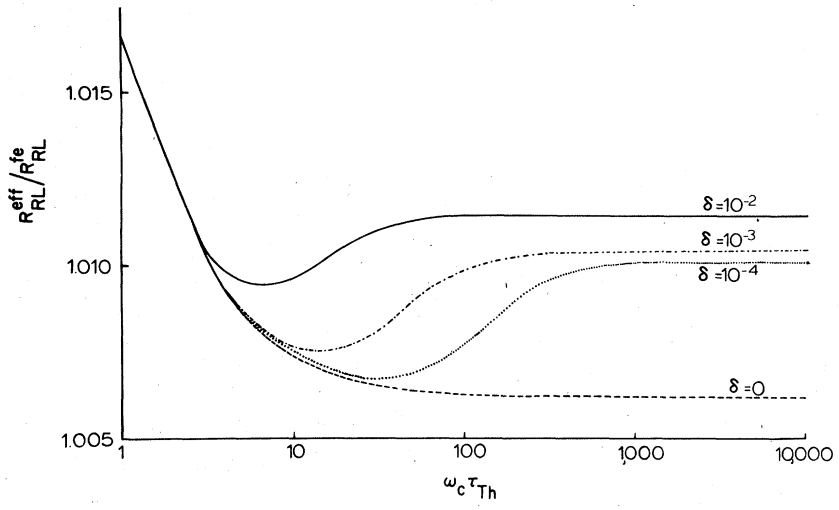

FIG. 7. The ratio of the effective Righi-Leduc coefficient to the free-electron Righi-Leduc coefficient (including the lattice conductivity) R_{RL}^{eff}/R_{RL}^{fe} vs $\omega_c\tau_{th}$. The $\delta = 0$ curve is also representative of the Hall coefficient R_H^{eff}/R_H^{fe}. (For spherical voids.)

the results compare with experimental data for the simple metals, and we offer suggestions to test the model.

Before discussing the results in detail, we address ourselves to two important questions: (i) How well does a free-electron model approximate a real metal? (ii) Since a void is a very gross inhomogeneity, how valid are the results discussed above, insofar as real metals are concerned?

The first question may be answered simply. The free-electron model provides an excellent approximation to the magnetic-field dependence of the conductivity of a real, simple metal in the high-field limit. Consider a cubic simple metal (for convenience) with the magnetic field parallel to a symmetry axis and $\hat{z}$. According to the semiclassical theory,[1] either of the two conductivity tensors can be written as

$$\begin{bmatrix} \frac{a^{xx}(T,c)}{H^2} & -\frac{ne}{H} & 0 \\ +\frac{ne}{H} & \frac{a^{xx}(T,c)}{H^2} & 0 \\ 0 & 0 & a^{zz}(T,c) \end{bmatrix}, \tag{40}$$

The coefficients a^{ii} are independent of the magnetic field but dependent on temperature (T) and purity (c). At any particular temperature, the a^{ii} are constant, and the conductivity tensor is essentially free-electron-like for $\omega_c\tau \gg 1$.

The second question is much more difficult to answer. Contraction voids can certainly exist in a metal, especially in those metals, such as the alkalis, which have large thermal expansion coefficients. However, the evidence is against there being large numbers of such voids in the specimens.[20] One must also consider surface effects. As pointed out by Sampsell and Garland,[15] surface roughness and indentations can act in a manner similar to voids and produce a linear electrical magnetoresistivity, and a very rough surface will provide a high "void density". Thus, at least for the alkalis, where smooth surfaces are difficult to obtain, the "void" model is meaningful. What of other forms of inhomogeneities? A useful approach is to examine the behavior of Eq. (28) in the opposite limit to that of a zero-conductivity inclusion, that is, to consider a highly conducting inclusion. There is a wide variety of possibilities. For example, in the electrical case, we might have a large field-independent conductivity in the inclusions, with the Hall terms similar to the bulk, or, we could allow the inclusion's conductivity to be field dependent. There are obviously other permutations possible, and, in each case, we must consider the thermal magnetoresistivity with the added complication of the field-independent lattice thermal conductivity. We have examined Eq. (28) in the light of these possibilities and reached a number of conclusions (some of which have already been noted by Stroud and Pan[16]).

For the electrical case. (i) Any spheroidal defect (and probably any shape of defect) leads to a linear transverse electrical magnetoresistance if, in the defect, either (i) σ'^{xx} and σ'^{yy} are field independent, or (ii) σ'^{xy} is proportional to $1/H$ and substantially different from σ^{xy}.

(ii) Only a defect of strictly zero conductivity leads to a strictly linear longitudinal electrical magnetoresistivity. Otherwise, saturation eventually occurs.

(iii) For either case (voids or highly conducting inclusions), the Köhler slopes are a constant of

$O(1)$ times f.

(iv) The fractional change in the Hall coefficient is never more than $O(f)$.

For the thermal case. (i) All defects, conducting or nonconducting, result in an extra term in the transverse thermal magnetoresistivity, which deviates from linearity at some value of $\omega_c\tau_{th}$ (which depends on δ), and then increases to saturation.

(ii) All defects, whether conducting or nonconducting, create an extra longitudinal thermal magnetoresistivity which saturates. The point of deviation from linearity depends on δ, and the extra resistance increases to saturation as a smooth, concave downward function of $\omega_c\tau$.

(iii) In the linear region, the Köhler slopes are identical to those of the electrical case.

(iv) The presence of voids changes the Righi-Leduc effect at most to $O(f)$.

Based on the above points, we reach a simple conclusion: The system we have considered, voids randomly distributed in a uniform background, appears to be representative of the effects of all types of inhomogeneous systems on the magnetoresistivity tensors. Furthermore, as mentioned above, the simple case of voids is amenable to experimental verification.

Comparisons between the predictions of the theory and experimental results in real metals reduce to comparisons with potassium. This is true for a number of reasons, the most important of which is that it is the only simple metal for which all of the electrical and thermal magnetotransport coefficients have been measured. (In the other simple metals, the experiments which have been done either are measurements of the transverse electrical magnetoresistance and the Hall effect or do not extend to sufficiently strong fields.) The situation in potassium is ambiguous. However, the experimental data can be interpreted in a manner which appears to eliminate the inhomogeneity hypothesis.

As mentioned above, it was the behavior of the linear transverse electrical magnetoresistivity of the simple metals which first prompted the inhomogeneity hypothesis. Voids or inclusion concentrations of $f\sim 10^{-4}$–10^{-3} can explain *most* of the electrical data in potassium. However, the large concentration of voids or inclusions needed to explain a Köhler slope of 10^{-2} is unreasonable. Furthermore, direct measurements of the lattice parameter of potassium at 4 K indicate that voids do not exist, at least to within one part in one thousand.[20] However, as indicated by Sampsell and Garland,[15] a rough surface constitutes a series of laterally displaced voids and, as such, can create an additional linear magnetoresistance. In potassium the surface could be rough enough to yield an effective $f\sim 10^{-2}$, particularly when combined with internal defects. (Such surface roughness is, however, unlikely in indium of aluminum.) Also, it is reasonable to expect a substantial density of conducting defects, such as strain and dislocation fields, grain boundaries, etc., in the specimen. Taken together, all of these could account for the large f that is needed to explain the data. The longitudinal electrical magnetoresistivity data, which should show saturation in the presence of conducting defects, does not provide us with any assistance. Although saturation is not observed, the experiments are ambiguous.[4,5] They indicate $\rho\propto H^n$ with $1\leq n\leq 2$ and do not extend to sufficiently strong fields.

The Hall coefficient data also requires a rather large f for an explanation. R_H has been found to be nearly 6% too large,[23] requiring $f\sim 6\times 10^{-2}$.

Thus, to say the least, the situation is unclear. On the evidence, the inhomogeneity hypothesis is a highly unlikely explanation but cannot be definitely ruled out. We now turn to the thermal data which ought always to show saturation. In potassium, the lattice thermal conductivity κ_g, has been found to be[24]

$$\kappa_g \simeq 3.3\times 10^{-2}T^2 , \tag{41}$$

and for the electronic thermal conductivity (in zero field) we may use[25]

$$\kappa_e \simeq [(5\times 10^{-4})/T + 1.5\times 10^{-5}T^2]^{-1} \tag{42}$$

as being representative for a specimen with a residual resistivity ratio of 6000. This yields a δ which varies between 2×10^{-5} and 2×10^{-4} in the temperature range 1–4 K. (Fletcher[8] has reported the possibility that κ_g may be four to five times larger than the above value.)

In this temperature range, values of $\omega_c\tau_{th}$ as large as 350 are easily reached in a potassium specimen of this purity. From Figs. 2, 3, or 6, we see that deviations from linearity should certainly be observable at $\omega_c\tau_{th}\sim 100$ for both the transverse and the longitudinal thermal magnetoresistivity.

Extensive measurements of the transverse thermal magnetoresistivity exist[7–9] and preliminary measurements of the longitudinal thermal magnetoresistivity are available.[9] In neither case is saturation observed. The transverse thermal magnetoresistivity is found to increase linearly and quadratically with field,

$$W_{xx}(H,T)T = W_0(0,T) + AH + BH^2 . \tag{43}$$

Both the linear and the quadratic terms are present to the highest fields used, with no sign of saturation. The presence of the quadratic term

may be construed as evidence that the inhomogeneity hypothesis is incorrect. There is no additional quadratic field-dependent thermal magnetoresistance due to the presence of the voids, see Figs. 2 or 6. Note that a quadratic term is expected independent of the presence of the voids.[24] This term, a result of the intermixing of magnetoconductivity tensor elements when $\kappa_g \neq 0$, has been shown to be too small to account for the data.[9,24] To fully explain the quadratic behavior in that manner, an unreasonably large[8,9] κ_g is required. Thus, the presence of the quadratic term would seem to indicate that the inhomogeneity hypothesis is incorrect. Again, however, the situation is not clear. It has been pointed out that the quadratic term might be a subtle form of measurement artifact,[8,21] and thus not part of the problem at hand. However, if that were true, we would still be left with a linear term in the transverse case and in the longitudinal case, with no sign of saturation, to values of $\omega_c\tau_{th} \approx 350$. The thermal Kohler slopes are four to five times larger than the electrical Köhler slopes, indicating the need for even larger concentrations of inhomogeneities. Finally, the measured Righi-Leduc coefficient is nearly in agreement with the free-electron value and, if anything, is smaller,[24] *not* larger than R_{RL}. We therefore conclude that it appears very likely that the magnetoresistivity anomalies in the simple metals (at least for potassium) cannot be explained by the inhomogeneity hypothesis. It will however be useful and instructive to extend the longitudinal measurements to much larger fields and measure the various transport coefficients on the same specimen.

As mentioned above, Beers *et al.*[19] recently measured the electrical magnetoresistivity of a high-purity indium specimen containing cylindrical voids. They essentially verified the above results for the electrical case. Such an experiment is clearly possible for the thermal magnetoresistivity and would be useful in verifying our results.

APPENDIX A: CYLINDRICAL INCLUSION ($\vec{J}_0 \perp \vec{H}$)

Let the cylindrical void of radius R_0 have its axis in the y direction, and let current be injected uniformly from infinity in the x direction, with magnitude J_0. The coordinate transformation to the twiddled system is defined by

$$x' = x^{1\prime} = \tilde{\alpha}\cosh\mu\cos\theta\,, \tag{A1}$$

$$y' = x^{2\prime} = y\,, \tag{A2}$$

$$z' = x^{3\prime} = \tilde{\alpha}\sinh\mu\sin\theta\,, \tag{A3}$$

$$\tilde{\alpha} = R_0(1-\Gamma)^{1/2} = R_0[(1-\gamma)/(1+\delta)]^{1/2}\,, \tag{A4}$$

and

$$(\tilde{x}^1, \tilde{x}^2, \tilde{x}^3) = (\mu, y, \theta)\,.$$

The appropriate solution of Laplace's equation for the temperature distribution is

$$\tilde{T}(\mu, y, \theta) = -(J_0/\kappa_0)(A\tilde{\alpha}\cosh\mu\cos\theta + By + C\cos\theta\, e^{-(\mu-\mu_0)})\,, \tag{A5}$$

with

$$A = (1+\rho)(1+\beta^2)[(1+\rho)^2+\beta^2]^{-1}\,, \tag{A6}$$

$$B = \beta(1+\beta^2)[(1+\rho)^2+\beta^2]^{-1}\,, \tag{A7}$$

$$C = R_0[\gamma(1+\delta)(1+\rho)]^{-1/2}\,, \tag{A8}$$

and

$$\sinh\mu_0 = [\Gamma/(1-\Gamma)]^{1/2}\,. \tag{A9}$$

The currents due to (A5) are given by Eq. (13) and have the forms

$$J_Q^x = J_0\{1 - e^{-(\mu-\mu_0)}[(\gamma+\delta)/(1-\gamma)]^{1/2}\Theta\}\,, \tag{A10}$$

$$J_Q^y = J_0 e^{-(\mu-\mu_0)}[\gamma/(\gamma+\delta)]^{1/2}\Theta\,, \tag{A11}$$

$$J_Q^z = -J_0 e^{\mu_0}[(1+\delta)/(1-\gamma)]^{1/2}\sin\theta\,\cos\theta\,\Phi\,, \tag{A12}$$

where

$$\Theta = (\sinh\mu\cos^2\theta - \cosh\mu\sin^2\theta)\Phi\,, \tag{A13}$$

and

$$\Phi^{-1} = (\sinh^2\mu\cos^2\theta + \cosh^2\mu\sin^2\theta)\,. \tag{A14}$$

The thermal gradients are immediate from Eq. (12),

$$\nabla_x T = \left(\frac{J_0}{\kappa_0}\right)\frac{(\gamma+\delta)(1+\beta^2)}{(1+\rho)^2+\beta^2} \times\left[1 - \frac{(1+\rho)^2+\beta^2}{(1+\rho)^2}\left(\frac{\gamma+\delta}{1-\gamma}\right)^{1/2} e^{-(\mu-\mu_0)}\Theta\right]\,, \tag{A15}$$

$$\nabla_y T = \left(\frac{J_0}{\kappa_0}\right)\frac{\beta(1+\beta^2)}{(1+\rho)^2+\beta^2}\,, \tag{A16}$$

and

$$\nabla_z T = -\left(\frac{J_0}{\kappa_0}\right)\frac{e^{\mu_0}}{(1+\delta)^{1/2}(1+\gamma)^{1/2}}\sin\theta\,\cos\theta\,\Phi\,. \tag{A17}$$

APPENDIX B: CYLINDRICAL INCLUSION ($\vec{J} \parallel \vec{H}$)

For this case, we have the same geometry as above with the incident current and the field in the z direction. Here the temperature distribution is

$$\tilde{T}(\mu, y, \theta) = -\left(\frac{J_0}{\kappa_0}\right)\frac{\Gamma^{1/2}R_0}{\gamma(1+\rho)}\sin\theta \times[(1-\Gamma)^{1/2}\sinh\mu + e^{-(\mu-\mu_0)}]\,. \tag{A18}$$

The currents and the thermal gradients are eval-

uated as above and have the forms

$$J_Q^x = -J_0[(\gamma+\delta)/(1-\gamma)]^{1/2} e^{\mu_0} \sin\theta \cos\theta \Phi , \quad \text{(A19)}$$

$$J_Q^y = -[\beta/(1+\rho)] J_Q^x , \quad \text{(A20)}$$

$$J_Q^z = J_0\{1 + [(1+\delta)/(1-\gamma)]^{1/2} e^{-(\mu-\mu_0)}\Theta\} , \quad \text{(A21)}$$

and

$$\nabla_x T = -\left(\frac{J_0}{\kappa_0}\right)\left(\frac{\gamma+\delta}{1-\gamma}\right)^{1/2} \frac{e^{\mu_0}}{\gamma(1+\rho)} \sin\theta\cos\theta\Phi , \quad \text{(A22)}$$

$$\nabla_y T = 0 , \quad \text{(A23)}$$

$$\nabla_z T = \left(\frac{J_0}{\kappa_0}\right)\frac{1}{1+\delta}\left[1 + \left(\frac{1+\delta}{1-\gamma}\right)^{1/2} e^{-(\mu-\mu_0)}\Theta\right] . \quad \text{(A24)}$$

APPENDIX C: SPHERICAL INCLUSION ($\vec{J}_0 \perp \vec{H}$)

Let the spherical void have a radius R_0 and let a uniform current of magnitude J_0 be injected along the x axis far from the void. The field is uniform and taken along the z axis. The coordinate transformation to the twiddled system is defined by

$$x' = x^{1\prime} = \tilde{\alpha} \cosh\eta \sin\theta \cos\phi , \quad \text{(A25)}$$

$$y' = x^{2\prime} = \tilde{\alpha} \cosh\eta \sin\theta \sin\phi , \quad \text{(A26)}$$

$$z' = x^{3\prime} = \tilde{\alpha} \sinh\eta \cos\theta , \quad \text{(A27)}$$

$$\tilde{\alpha} = R_0(1-\Gamma)^{1/2} , \quad \text{(A28)}$$

and

$$(\tilde{x}^1, \tilde{x}^2, \tilde{x}^3) = (\eta, \theta, \phi)$$

are oblate spheroidal coordinates. The appropriate solution of Laplace's equation for the temperature distribution is

$$\tilde{T}(\eta,\theta,\phi) = (J_0/\kappa_0)\sin\theta[A\cosh\eta(\cos\phi + \tilde{\beta}\sin\phi) + Q_1^1(i\sinh\eta) \times (C\cos\phi + D\sin\phi)] , \quad \text{(A29)}$$

where

$$A = -\tilde{\alpha}[\tilde{\gamma}(1+\tilde{\beta}^2)]^{-1} , \quad \text{(A30)}$$

$$D = \frac{\tilde{\alpha}}{\tilde{\gamma}}\left(\frac{\Gamma}{1-\Gamma}\right)^{1/2} \tilde{\beta}\,\Gamma^{1/2} Q_1^1(i\sinh\eta_0) \times \left[\left(\frac{dQ_1^1}{d\eta}\bigg|_{\eta_0}\right)^2 + \tilde{\beta}^2\Gamma(Q_1^1|_{\eta_0})^2\right]^{-1} , \quad \text{(A31)}$$

$$C = \frac{dQ_1^1}{d\eta}\bigg|_{\eta_0} [\tilde{\beta}\,\Gamma^{1/2} Q_1^1(i\sinh\eta_0)]^{-1} D , \quad \text{(A32)}$$

where

$$Q_1^1(z) = (z^2-1)^{1/2}\frac{d}{dz}Q_1(z) , \quad \text{(A33)}$$

with $Q_1(z)$ the associated Legendre function of the second kind given by

$$Q_1(z) = \tfrac{1}{2} z \ln[(z+1)/(z-1)] - 1 . \quad \text{(A34)}$$

The currents and the gradients have the forms

$$J_Q^x = -(J_0\tilde{\gamma}/\tilde{\alpha}\Sigma)\{\sinh\eta\sin^2\theta\cos\phi[A(N+\tilde{\beta}O)\sinh\eta + CP + DR] + \cosh\eta\cos^2\theta\cos\phi[A(N+\tilde{\beta}O)\cosh\eta + Q_1^1(CN+DO)] - \cosh\eta\sin\theta\sin\phi(AF+BG+CH+DI)\} , \quad \text{(A35)}$$

$$J_Q^y = -(J_0\tilde{\gamma}/\tilde{\alpha}\Sigma)\{\sinh\eta\sin^2\theta\sin\phi[A(N+\tilde{\beta}O)\sinh\eta + CP + DR] + \cosh\eta\cos^2\theta\sin\phi[A(N+\tilde{\beta}O)\cosh\eta + Q_1^1(CN+DO)] + \cosh\eta\sin\theta\cos\phi(AF+BG+CH+DI)\} , \quad \text{(A36)}$$

$$J_Q^z = -(J_0\tilde{\gamma}/\tilde{\alpha}\Gamma^{1/2}\Sigma)[\cosh\eta(CP+DR) - \sinh\eta\, Q_1^1(CN+DO)]\sin\theta\cos\theta , \quad \text{(A37)}$$

and

$$\nabla_x T = \frac{1}{\tilde{\alpha}\Sigma}\left(\frac{J_0}{\kappa_0}\right)\left[A(\cos^2\phi + \tilde{\beta}\sin\phi\cos\phi)\Sigma + (C\cos^2\phi + D\sin\phi\cos\phi)\left(\frac{dQ_1^1}{d\eta}\sinh\eta\sin^2\theta + Q_1^1\cosh\eta\cos^2\theta\right)\right] - \frac{1}{\tilde{\alpha}X}\left(\frac{J_0}{\kappa_0}\right)\sin\theta\sin\phi[\cosh\eta A(\tilde{\beta}\cos\phi - \sin\phi) + Q_1^1(D\cos\phi - C\sin\phi)] , \quad \text{(A38)}$$

$$\nabla_y T = \frac{1}{\tilde{\alpha}\Sigma}\left(\frac{J_0}{\kappa_0}\right)\left[A(\sin\phi\cos\phi + \tilde{\beta}\sin^2\phi)\Sigma + (C\cos\phi\sin\phi + D\sin^2\phi)\left(\frac{dQ_1^1}{d\eta}\sinh\eta\sin^2\theta + Q_1^1\cosh\eta\cos^2\theta\right)\right] + \frac{1}{\tilde{\alpha}X}\left(\frac{J_0}{\kappa_0}\right)\sin\theta\cos\phi[\cosh\eta A(\tilde{\beta}\cos\phi - \sin\phi) + Q_1^1(D\cos\phi - C\sin\phi)] , \quad \text{(A39)}$$

$$\nabla_z T = -\frac{\Gamma^{1/2}}{\tilde{\alpha}\Sigma}\left(\frac{J_0}{\kappa_0}\right)\sin\theta\cos\theta\left(\frac{dQ_1^1}{d\eta}\cosh\eta - Q_1^1\sinh\eta\right)(C\cos\phi + D\sin\phi) , \quad \text{(A40)}$$

with

$$X = \cosh\eta\sin\theta , \quad \text{(A41)}$$

$$\Sigma = \sinh^2\eta\sin^2\theta + \cosh^2\eta\cos^2\theta , \quad \text{(A42)}$$

$$N = \cos\phi - \tilde{\beta}\sin\phi , \quad \text{(A43)}$$

$$O = \sin\phi + \tilde{\beta}\cos\phi , \quad \text{(A44)}$$

$$P=\frac{dQ_1^1}{d\eta}\cos\phi-\tilde{\beta}\,Q_1^1\tanh\eta\,\sin\phi\,, \tag{A45}$$

$$R=\frac{dQ_1^1}{d\eta}\sin\phi+\tilde{\beta}\,Q_1^1\tanh\eta\cos\phi\,, \tag{A46}$$

$$F=-\tilde{\beta}\tanh\eta\,\sinh\eta\sin\theta\cos\phi - \tilde{\beta}\cosh\eta\cot\theta\cos\theta\cos\phi - \Sigma X^{-2}\cosh\eta\sin\theta\sin\phi\,, \tag{A47}$$

$$G=-\tilde{\beta}\tanh\eta\sinh\eta\sin\theta\sin\phi - \tilde{\beta}\cosh\eta\cot\theta\cos\theta\,\sin\phi + \Sigma X^{-2}\cosh\eta\sin\theta\,\cos\phi\,, \tag{A48}$$

$$H=-\tilde{\beta}\frac{dQ_1^1}{d\eta}\tanh\eta\,\sin\theta\,\cos\phi-\tilde{\beta}Q_1^1\cot\theta\cos\theta\,\cos\phi - \Sigma X^{-2}\,Q_1^1\sin\theta\,\sin\phi\,, \tag{A49}$$

and

$$I=-\tilde{\beta}\frac{dQ_1^1}{d\eta}\tanh\eta\sin\theta\sin\phi-\tilde{\beta}Q_1^1\cot\theta\cos\theta\sin\phi + \Sigma X^{-2}Q_1^1\sin\theta\cos\phi\,. \tag{A50}$$

APPENDIX D: SPHERICAL INCLUSIONS ($\vec{J}\parallel\vec{H}$)

Let the spherical void have a radius R_0 and let a uniform current of magnitude J_0 be injected along the field which is chosen to be in the z direction. The temperature distribution, the currents, and the gradients have the forms

$$\tilde{T}(\eta,\theta,\phi)=\left(\frac{J_0}{\kappa_0}\right)\frac{R_0(1-\Gamma)^{1/2}}{\gamma(1+\rho)} \times[MQ_1(i\sinh\eta)-\Gamma^{1/2}\sinh\eta]\cos\theta\,, \tag{A51}$$

$$J_Q^x=J_0M\sin\theta\cos\theta\,U[\cos\phi+\beta(1+\rho)^{-1}\sin\phi]N, \tag{A52}$$

$$J_Q^y=J_0M\sin\theta\cos\theta\,U[\sin\phi-\beta(1+\rho)^{-1}\cos\phi]N, \tag{A53}$$

$$J_Q^z=J_0(1-MPU\Gamma^{-1/2})\,, \tag{A54}$$

and

$$\nabla_x T=\left(\frac{J_0}{\kappa_0}\right)\frac{M}{\gamma(1+\rho)}\sin\theta\,\cos\theta\cos\phi\,UN\,, \tag{A55}$$

$$\nabla_y T=\left(\frac{J_0}{\kappa_0}\right)\frac{M}{\gamma(1+\rho)}\sin\theta\cos\theta\sin\phi\,UN\,, \tag{A56}$$

$$\nabla_z T=\left(\frac{J_0}{\kappa_0}\right)\frac{\Gamma}{\gamma(1+\rho)}(1-MPU\,\Gamma^{-1/2})\,, \tag{A57}$$

with

$$M=\sinh\eta_0\Big/\left(\frac{dQ_1}{d\eta}\right)_{\eta_0}\,, \tag{A58}$$

$$N=Q_1(i\sinh\eta)\cosh\eta-\frac{dQ_1(i\sinh\eta)}{d\eta}\sinh\eta\,, \tag{A59}$$

$$P=\frac{dQ_1(i\sinh\eta)}{d\eta}\cosh\eta\cos^2\theta + Q_1(i\sinh\eta)\sinh\eta\sin^2\theta\,, \tag{A60}$$

$$\sinh\eta_0=[\Gamma/(1-\Gamma)]^{1/2}\,, \tag{A61}$$

and

$$U^{-1}=\sinh^2\eta\sin^2\theta+\cosh^2\eta\cos^2\theta\,. \tag{A62}$$

[1] I. M. Lifshitz, M. Ya. Azbel, and M. I. Kaganov, Zh. Eksp. Teor. Fiz. 30, 200 (1955) [Sov. Phys. JETP 3, 143 (1956)]; Zh. Eksp. Teor. Fiz. 31, 63 (1956) [Sov. Phys. JETP 4, 41 (1957)].

[2] H. Taub, R. L. Schmidt, B. W. Maxfield, and R. Bowers, Phys. Rev. B 4, 1134 (1971), and references therein.

[3] J. Babiskin and P. G. Siebenmann, Phys. Rev. Lett. 27, 1361 (1971).

[4] J. S. Lass, J. Phys. C 3, 1926 (1970).

[5] A. M. Simpson, J. Phys. F 3, 1471 (1973).

[6] See for example, F. R. Fickett, Phys. Rev. B 3, 1941 (1971).

[7] R. S. Newrock and B. W. Maxfield, J. Low Temp. Phys. 23, 119 (1976).

[8] R. Fletcher, Phys. Rev. Lett. 32, 930 (1974).

[9] P. J. Tausch, R. S. Newrock, and W. Mitchel, Phys. Rev. B 20, 501 (1979).

[10] The various proposed explanations are reviewed in Refs. 2 and 7. Also, R. S. Newrock (unpublished).

[11] J. A. Delaney and A. B. Pippard, Rep. Prog. Phys. 35, 677 (1972).

[12] H. J. Lippmann and F. Kuhrt, Z. Naturforsch. Teil A 13, 462 (1958).

[13] H. H. Jensen and H. Smith, J. Phys. C 5, 2867 (1972).

[14] P. M. Martin, J. B. Sampsell, and J. C. Garland, Phys. Rev. B 15, 5598 (1977). See also, references in Ref. 15.

[15] J. B. Sampsell and J. G. Garland, Phys. Rev. B 13, 583 (1976).

[16] D. Stroud and F. P. Pan, Phys. Rev. B 13, 1434 (1976).

[17] C. Herring, J. Appl. Phys. 31, 1939 (1960); R. Landauer, J. Appl. Phys. 23, 779 (1952); H. Stachowick, Physica (Utrecht) 45, 481 (1970). See also, references in Ref. 15.

[18] C. J. Beers, J. C. M. Von Dangen, H. Van Kempen, and P. Wyder, Phys. Rev. Lett. 40, 1194 (1978).

[19] R. Landauer, AIP Conf. Proc. 40, 1 (1977) and references therein.

[20] D. R. Schouten and C. A. Swenson, Phys. Rev. B 10, 2175 (1974).

[21] R. Fletcher (unpublished).

[22] F. P. Esposito, R. S. Newrock, and K. Loeffler, Phys. Rev. Lett. 41, 818 (1978).

[23] See, for example, D. E. Chimenti and B. W. Maxfield, Phys. Rev. B 7, 3501 (1973).

[24] P. Tausch and R. S. Newrock, Phys. Rev. B 16, 5381 (1977).

[25] R. S. Newrock and B. W. Maxfield, Phys. Rev. B 7, 1783 (1973).